

Electronic and Vibrational Polarizabilities and Hyperpolarizabilities of Azoles: A Comparative Study of the Structure–Polarization Relationship

Karl Jug* and Sandro Chiodo

Theoretische Chemie, Universität Hannover, Am Kleinen Felde 30, 30167 Hannover, Germany

Patrizia Calaminici

Departamento de Química, CINVESTAV, Avenida Instituto Politecnico Nacional, 2508, A.P. 14-740 Mexico D.F. 07000, Mexico

Aggelos Avramopoulos and Manthos G. Papadopoulos*

Institute of Organic and Pharmaceutical Chemistry, National Hellenic Research Foundation, 48 Vas. Constantinou, Athens 11635, Greece

Received: November 11, 2002; In Final Form: February 18, 2003

Density functional theory (DFT) is used to study the static electronic dipole moments, polarizabilities, polarizability anisotropies, and first- and second-order hyperpolarizabilities of azoles. These properties are obtained with a finite field approach implemented in the DFT program ALLCHEM. The calculations were of all-electron type using a local exchange correlation functional. To investigate the dependence of polarizabilities and first- and second-order hyperpolarizabilities on the geometries, all structures were optimized with ALLCHEM and MSINDO. The influence of the substituted atoms on the properties is discussed. The vibrational contributions to the above properties of the considered compounds have also been computed using SCF theory and analytic property derivatives. Several methods (basis sets and approaches to determine the electron correlation contribution) have been employed to confirm the adequacy of the method, which was used. The electronic and vibrational properties are connected with various aspects of the electronic and vibrational structure and they are rationalized by simple concepts (resonance structures) and properties (fragments, derivatives). The present results are in satisfactory agreement with the available experimental data.

1. Introduction

Five-membered heterocycles have been a favored class of compounds of chemistry research for many years. Their structure and stability, their aromaticity, and their reactivity have been comprehensively reviewed.¹ Aromatic species include pyrrole, furan, and thiophene. Further substitution in the ring generates a variety of other heterocycles, among which the azoles represent a most prominent group. It is interesting to see how the properties change upon this specific substitution of CH fragments by N atoms. Although much has been said about the aromaticity of such compounds, much less is known about their polarizability. In nonlinear optics^{2,3} hyperpolarizabilities are the focus of attention because of their importance for new materials and devices. Nonlinear optical processes in π -electron organic systems have attracted considerable interest because their understanding has also led to new theoretical insight.² In this sense it is hoped that a systematic investigation of polarizabilities and second hyperpolarizabilities of azoles furnishes new information and better understanding of these properties.

The focus of this work is therefore not the development of new methods, but a comparative study of the structure–polarization relationship for azoles. In this respect papers by Keshari et al.,⁴ El-Bakali Kassimi et al.,^{5–7} and Kamada et al.⁸ on heterocyclic structures are relevant. Keshari et al.⁴ present ab initio time-dependent coupled perturbed Hartree–Fock–

Rootaan studies of basic heterocyclic structures, among them pyrrole, furan, and thiophene. They report linear polarizability α , first hyperpolarizability β , and second hyperpolarizability γ for these compounds. The structures were optimized at the SCF level with a 4-31G* basis set. This basis set was considered inadequate for the calculation of polarizabilities and hyperpolarizabilities. They undertook a basis set study for a smaller set of compounds including thiophene with basis sets ranging from STO-3G to 4-31G plus field-induced polarization functions (FIP). Their best results for α were with the 4-31G + FIP set. Their calculated value for thiophene was 8% too small. The agreement of calculated γ values with the experimental values was rather poor because of the choice of an outdated experimental value. In a series of papers on azoles El-Bakali Kassimi et al.^{5–7} reported static dipole polarizabilities α with various basis sets on the uncoupled and coupled Hartree–Fock level and the MP2 level. In the first paper⁵ they do not list the experimental values in the tables, but from the text it is apparent that their best results are on the MP2 level with a double- ζ plus polarization basis set. Their best agreement with the experimental values is clearly better than that by Keshari et al. No β or γ values are reported. In a more recent paper Kamada et al.⁸ report static polarizabilities α and hyperpolarizabilities β and γ for furan and thiophene. α and β values were calculated on the Hartree–Fock level by the coupled perturbed Hartree–Fock method, whereas γ values were determined on the Hartree–Fock level by finite field methods. Correlation effects were

* Corresponding authors.

TABLE 1. Comparison of $\bar{\beta}$ and $\bar{\gamma}$ Values (au) with Various Methods

compd	$\bar{\beta}$	$\bar{\gamma}$	compd	$\bar{\beta}$	$\bar{\gamma}$	compd	$\bar{\beta}$	$\bar{\gamma}$
HF	-9.57 ^a	665 ^a	H ₂ O	-22.41 ^a	2118 ^a	NH ₃	-34.10 ^a	4595 ^a
	-9.23 ^b	1000 ^b		-25.70 ^b	3200 ^b		-55.40 ^b	8000 ^b
	-7.30 ^c	560 ^c		-18.00 ^c	1800 ^c		-34.30 ^c	4200 ^c

^a Reference 9. ^b Reference 18. ^c Reference 19.

investigated at the MP2 and MP4 level and on the coupled cluster (CC) level. Three basis sets on the 6-31G level plus polarization functions and diffuse functions were used. There is an emphasis on the basis set and level dependence. The agreement with the experimental values is between about 2 and 11% for furan and between about 2 and 12% for thiophene. The best agreement is on the CCSD(T) level. For γ values the best agreement is again on the CCSD(T) level. The best value for furan differs by 1.3% from the experimental value, but for thiophene the calculated CCSD(T) γ value is too low by about 23%.

In the following we present results on α , β , and γ values for a more comprehensive set of compounds on a level of accuracy which is as good or better than the best reported values. The emphasis is not on trends in basis sets, rather trends in compounds. We also add a portion on the significance of vibrational contributions which is not contained in the above-discussed papers.

2. Computational Method

In a series of previous papers⁹⁻¹¹ we demonstrated the suitability of the density functional theory (DFT) program ALLCHEM¹² for the calculation of polarizabilities and hyperpolarizabilities of small- and medium-size molecules and clusters. The computational details can be found there. In this paper we repeat only the most essential features. ALLCHEM is a DFT program which uses auxiliary functions^{13,14} and an adaptive grid.¹⁵ The calculations were performed in the local density approximation (LDA) using the exchange correlation functionals proposed by Vosko, Wilk, and Nusair.¹⁶ To obtain reliable values for the polarizabilities, a triple- ζ plus valence polarization (TZVP) basis set was used, which was augmented with field-induced polarization (FIP) functions by Zeiss et al.¹⁷

We consider three examples, HF, H₂O, and NH₃, to demonstrate that the basis set is of great importance. Thus, the results of Calaminici et al.⁹ are compared with those of van Gisbergen et al.¹⁸ and Sekino and Bartlett.¹⁹ These data are presented in Table 1. We note that Gisbergen et al. employed a large STO basis set, which has not been designed or optimized for hyperpolarizability calculations. Thus, their hyperpolarizability values may differ from those computed by Calaminici et al. or Sekino and Bartlett. Both groups use basis sets designed for polarizability calculations. Differences by a factor of 2 may occur, although both Calaminici et al. and Gisbergen et al. use the LDA method. Another paper by Aiga et al.²⁰ does not contain any data and can therefore not be included in the comparison.

The structures of all studied compounds were fully optimized. The electronic properties were calculated for the optimized structures. Polarizabilities and hyperpolarizabilities were calculated via the finite field method by Kurtz et al.,²¹ which was implemented in the ALLCHEM program. We have also computed analytically²² the polarizability and first hyperpolarizability of furan, isoxazole, thiazole, pyrazole, and imidazole, to check the accuracy of our finite field procedure. The largest discrepancy between the numerically and analytically computed

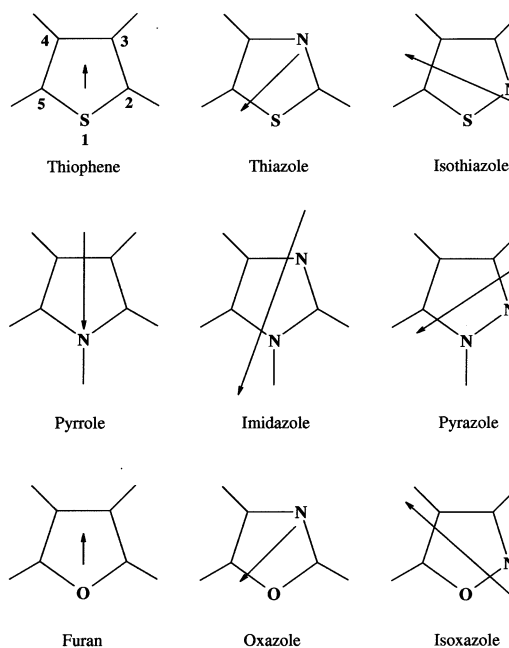


Figure 1. Structure and dipole moment of thiophene, pyrrole, and furan and their azole derivatives.

polarizabilities and first hyperpolarizabilities (their absolute value has been considered) is 0.42% and 0.82%, respectively. So for the polarizability and the first hyperpolarizability, our numerical technique is associated with no significant loss of accuracy in comparison to the analytical approach.²² For the second hyperpolarizability, we may have a bit larger discrepancy from the results produced by an analytical method. However, we expect that this discrepancy will not be large enough to affect the findings of our comparative study.

To test the suitability of semiempirically optimized molecular structures for the calculation of molecular polarizabilities with DFT methods, we have also optimized the studied azoles with the new semiempirical program MSINDO,²³⁻²⁵ which is based on an improved modification of the SINDO1 program.²⁶

3. Electronic Contributions for Azoles

3.1. Structures and Dipole Moments. The structures of thiophene, pyrrole, and furan and the considered series of azoles, diazoles, and triazoles are illustrated in Figures 1 and 2. These figures contain also the direction and relative magnitude of the permanent dipole moments. The structures were optimized with ALLCHEM and MSINDO. The calculated bond lengths and bond angles are compared with experimental values.²⁷⁻³³ The structural data are available as Supporting Information. The agreement between the LDA/DZVP optimized and the experimental geometries is very good. The largest deviation is 0.043 Å. The MSINDO values are of lesser accuracy with a maximum deviation of 0.112 Å. On the other hand, the MSINDO values for CH bond lengths show better agreement with experiment than the DFT values.

All electric property values were calculated at the LDA level for both DFT and MSINDO optimized geometries. The purpose was to investigate the influence of the level of structure optimization, DFT versus semiempirical, on the electric properties. The permanent dipole moments of the considered molecules are listed in Table 2. Their relative orientations are shown in Figures 1 and 2. For both DFT and MSINDO structures the DFT values of the dipole moments are in good or very good agreement with experimental values in the gas phase.^{32,34-38}

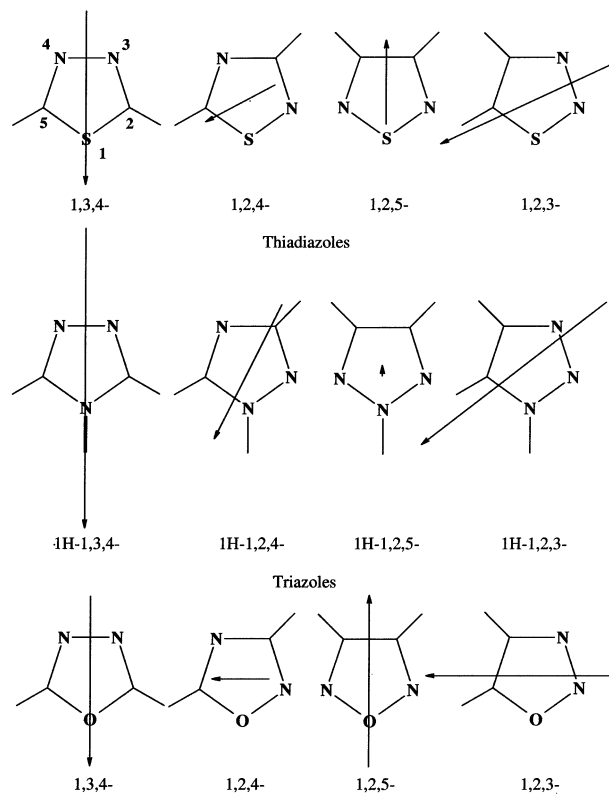


Figure 2. Structure and dipole moment of diazoles.

3.2. Polarizabilities and Polarizability Anisotropies. For the calculation of the static polarizabilities $\bar{\alpha}$ and polarizability anisotropies $|\Delta\alpha|$ a Cartesian coordinate system is chosen with the origin in the center of mass and the z axis along the direction of the permanent dipole moment of the molecule.

From the polarizability tensor we obtain

$$\bar{\alpha} = \frac{1}{3}(\alpha_{xx} + \alpha_{yy} + \alpha_{zz})$$

$$|\Delta\alpha|^2 = \frac{3 \text{tr } \alpha^2 - (\text{tr } \alpha)^2}{2}$$

$$= \frac{1}{2}[(\alpha_{xx} - \alpha_{yy})^2 + (\alpha_{xx} - \alpha_{zz})^2 + (\alpha_{yy} - \alpha_{zz})^2] \quad (1)$$

Table 3 lists the calculated and experimental polarizabilities and polarizability anisotropies.^{39–43} From the several experimental values reported for thiophene, pyrrole, and furan the oldest value³⁹ seems the least accurate for the $\bar{\alpha}$ values. For the rest, the agreement between calculation and experiment is very good. This is also the case for imidazole and pyrazole. This is true for both values obtained with DFT and MSINDO geometries. To substantiate the quality of our results, we repeated the calculations for α and $|\Delta\alpha|$ for several azoles (thiophene, pyrrole, imidazole, pyrazole, and furan) with the exchange-correlation functionals PW86P86⁴⁴ and BLYP.⁴⁵ The maximum differences for α and $|\Delta\alpha|$ with the two nonlocal functionals compared to our local VWN calculations did not exceed 1.2%. We can therefore expect that our calculated values with no experimental counterparts are equally reliable. It should be mentioned here that ab initio calculations on polarizabilities of pyrrole,⁵ furan,⁶ thiophene,⁷ and their azoles have been reported. The emphasis was on the basis set dependence of dipole moments and polarizabilities. From these papers it is apparent that a large basis set and correlation is needed to arrive at reliable values.

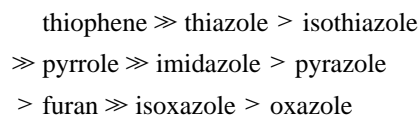
TABLE 2. Permanent Dipole Moment μ (Debye)^g of Azoles

molecule	DFT geometries	MSINDO geometries	experiment
thiophene	0.478	0.613	0.533 ± 0.0005 ^a
thiazole	1.664	1.623	1.61 ± 0.03 ^a
isothiazole	2.503	2.602	2.44 ± 0.2 ^a
pyrrole	1.936	1.833	1.74 ± 0.02 ^a
imidazole	3.840	3.823	3.8 ± 0.4 ^a
pyrazole	2.334	2.356	2.21 ^a
furan	0.606	0.821	0.661 ± 0.006 ^b
oxazole	1.636	1.580	1.50 ^a
isoxazole	3.015	3.130	2.90 ^a
thiadiazoles			
1,3,4-	3.358	3.274	3.28 ± 0.03 ^a
1,2,4-	1.532	1.458	1.49 ^c
1,2,5-	1.554	1.829	1.565 ± 0.015 ^a
1,2,3-	3.615	3.313	3.59 ± 0.13 ^d
triazoles			
1H-1,3,4-	5.813	5.744	
1H-1,2,4-	2.923	2.844	2.72 ± 0.12 ^a
1H-1,2,5-	0.122	0.317	0.22 ^e
1H-1,2,3-	4.552	4.408	4.38 ^e
oxadiazoles			
1,3,4-	3.280	3.185	3.04 ± 0.04 ^f
1,2,4-	1.151	1.086	1.2 ± 0.3 ^a
1,2,5-	3.335	3.630	3.38 ± 0.04 ^a
1,2,3-	3.667	3.541	

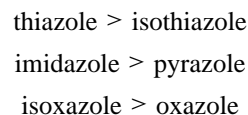
^a Reference 34. ^b Reference 35. ^c Reference 36. ^d Reference 37. ^e Reference 38. ^f Reference 39. ^g 1 au = 2.54174 D = 8.47831 × 10⁻³⁰ C m.

For the $|\Delta\alpha|$ values the agreement among the experimental values is not so good. Consequently, there are also deviations between the calculated and some experimental values. For example, the agreement between the DFT and MSINDO based values with the experimental values measured by Calderbank et al.⁴³ is mediocre for pyrrole and its azoles. However, these authors have imposed severe simplifications on their evaluation. They consider the N–H bond in imidazole and pyrazole as the principal axis, and they equate the in-plane polarizabilities $\alpha_{||} = \alpha_{\perp}$ for pyrrole and pyrazole and assume the same out-of-plane polarizability for imidazole and pyrazole. For pyrrole they report $\alpha_{||} = \alpha_{\perp} = 61.26$ au, whereas we obtained $\alpha_{||} = 62.63$ au and $\alpha_{\perp} = 65.70$ au.

From a comparison of the calculated $\bar{\alpha}$ values in Table 3, we obtain the following order:



It is obvious that the present ordering is in principle determined by the atomic contributions $\bar{\alpha}_S = 32.01$ au, $\bar{\alpha}_C = 12.86$ au, $\bar{\alpha}_N = 7.65$ au, and $\bar{\alpha}_O = 5.50$ au. Substitution of S by NH is accompanied by a significant decrease in $\bar{\alpha}$ of about 9 au. Further substitution of NH by O leads to another decrease of about 6 au. Replacement of CH by N is accompanied by a decrease of approximately 5 au. To understand the relative order of the azoles,



we have to consider the resonance structures in Figure 3. The separation of charge generated by a push–pull effect of the heteroatoms in an electric field increases the molecular polar-

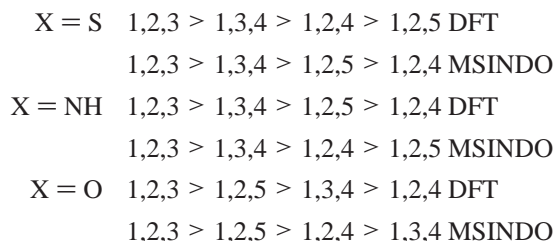
TABLE 3. Average Polarizabilities $\bar{\alpha}$ and Polarizability Anisotropies $|\Delta\alpha|$ [au]^h of Azoles with DFT and MSINDO Optimized Geometries

	DFT geometries		MSINDO geometries		experiment	
	$\bar{\alpha}$	$ \Delta\alpha $	$\bar{\alpha}$	$ \Delta\alpha $	$\bar{\alpha}$	$ \Delta\alpha $
thiophene					60.6 ^a	23.1 ^a
					65.2 ± 2.1 ^b	21.6 ± 3.4 ^b
					66.1 ^c	
					64.9 ± 0.6 ^d	31.9 ± 7.9 ^d
thiazole	59.99	29.76	60.63	30.21		
isothiazole	59.48	30.02	60.61	31.32		
pyrrole	55.77	25.33	55.47	24.84	53.5 ^a	22.3 ^a
imidazole	50.58	24.63	50.66	24.43	55.8 ^e	16.7 ^e
pyrazole	50.00	23.58	50.28	23.71	50.9 ^e	16.7 ^e
					48.8 ^a	20.7 ^a
furan	49.70	22.77	49.55	22.39	49.1 ± 2.2 ^b	15.3 ± 4.4 ^b
					50.63 ^g	49.1 ± 0.5 ^d
oxazole	44.49	21.55	44.78	21.45		
isoxazole	44.62	21.35	45.10	21.70		
thiadiazoles						
1,3,4-	55.42	28.42	56.36	29.03		
1,2,4-	54.32	27.90	55.74	29.28		
1,2,5-	54.06	29.26	56.06	31.37		
1,2,3-	56.08	30.05	57.44	31.86		
triazoles						
1H-1,3,4-	45.39	23.09	45.85	23.28		
1H-1,2,4-	44.61	22.25	45.35	22.72		
1H-1,2,5-	44.64	21.69	45.34	22.25		
1H-1,2,3-	45.58	22.52	45.97	22.68		
oxadiazoles						
1,3,4-	39.39	19.84	40.11	20.22		
1,2,4-	39.27	19.63	40.14	20.23		
1,2,5-	39.95	19.50	40.79	20.28		
1,2,3-	40.65	20.11	40.89	20.00		

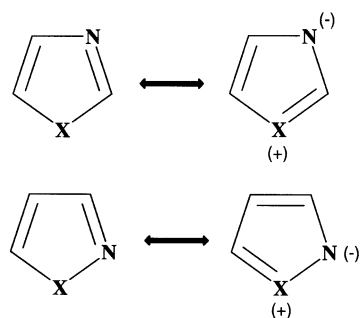
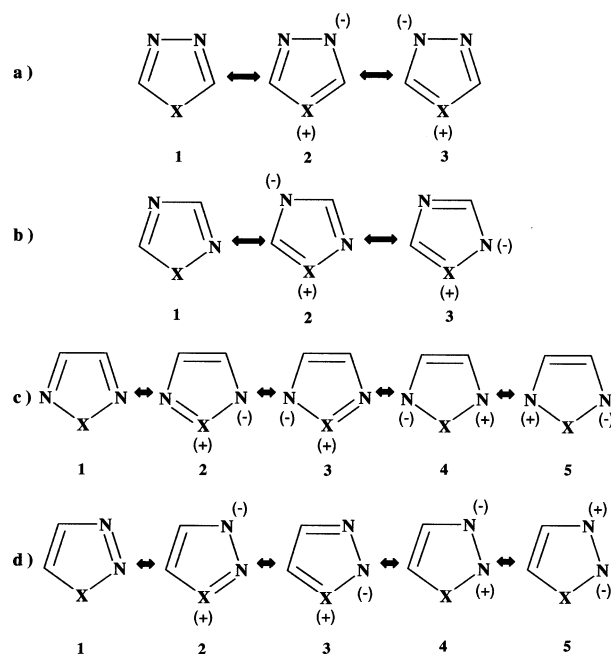
^a Reference 39. ^b Reference 40. ^c Reference 41. ^d Reference 42. ^e Reference 43. ^f $\bar{\alpha}(-\omega;\omega)$, $\lambda = 790$ nm, pure vibrational contribution -0.015 au. ^g $\bar{\alpha}(-\omega;\omega)$, $\lambda = 790$ nm, pure vibrational contribution -0.015 au. ^h 1 au = 1.48176×10^{-25} cm³ = 1.64867×10^{-41} C²·m²/J.

izability. Assuming equal charge separation for the azole and its isoform, the larger distance between the positive and negative charge in the isoform should lead to a larger polarizability. This is indeed true for isothiazole and pyrazole. But this order is reversed for isoxazole and oxazole. Here, we must consider that charge separation $X^+ \rightarrow N^-$ is largest for $X = S$, less for $X = NH$, and poor for $X = O$. In the latter case, the smaller distance is actually more favorable for the charge transfer than the larger distance because the system can avoid charge transfer from O to N best at large distances between these two atoms.

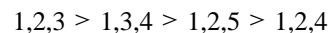
Replacement of a second C–H group with nitrogen leads to a further reduction of the azole $\bar{\alpha}$ values. This means that the diazoles have smaller $\bar{\alpha}$ values than the corresponding azoles. If the various isomers are compared, the following sequences can be seen for $\bar{\alpha}$ of diazoles and triazoles.



To explain these trends, we show the various resonance structures and the charge separation in Figure 4. As we have already seen for the azoles of thiophene and pyrrole, the larger distance favors the larger $\bar{\alpha}$ value. This would mean that the

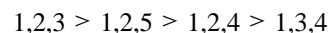
**Figure 3.** Resonance structures of azoles.**Figure 4.** Resonance structures of diazoles.

structures 1,2,3 are favored over 1,2,5 and 1,3,4 over 1,2,4. The charge separation effect is enhanced by an increasing number of resonance structures. This increase leads to a larger pull–push effect, that is, to a larger variation of the induced dipole moment (Figure 5) and consequently to a larger polarizability. For $X = S$ the sequence



would be natural because 1,2,3 and 1,2,5 have five resonance structures compared to three for 1,3,4 and 1,2,4. However, the weight of resonance structures 4c and 5c should be lower than that of 2c and 3c because the former have lost part of their π -electron conjugation. This holds also for 4d and 5d. It can be expected that this description is valid for $X = NH$, too.

However, for $X = O$ the smaller distance between O and N was more effective in the case of oxazole. This would favor 1,2,3 and 1,2,5 as well as 1,2,4 over 1,3,4. The first two have the higher number of resonance structures compared with the third isomer. 1,2,3 has three resonance structures with nearest-neighbor charge separation, whereas 1,2,5 has only two. The natural sequence for $X = O$ would therefore be



A more refined consideration would have to consider the actual distances in the molecules as calculated by the DFT and MSINDO methods.

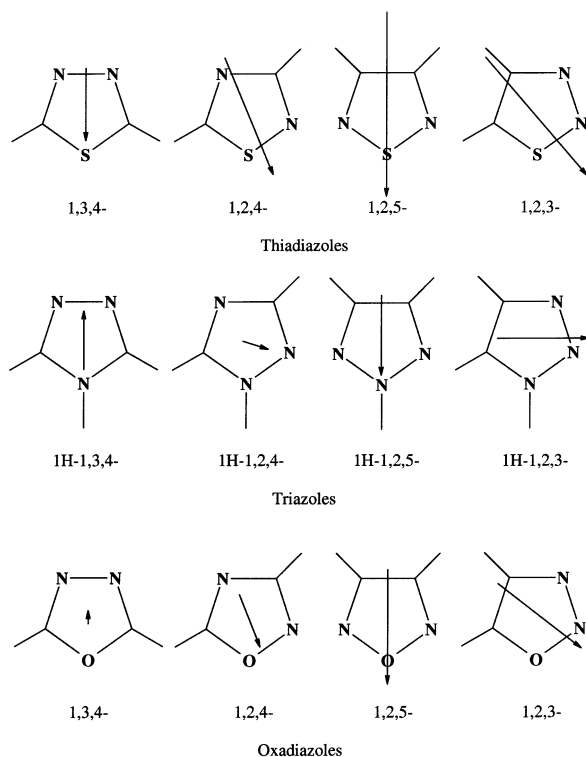


Figure 5. Induced dipole moments of diazoles and triazoles.

3.3. First Hyperpolarizabilities. The calculated static β components permit the calculation of the mean first hyperpolarizability $\bar{\beta}$, which may be defined as nine-fifths of the partial derivative of the mean polarizability $\bar{\alpha}$ with respect to field F_z oriented along the direction of the permanent dipole moment:

$$\bar{\beta} = \frac{9}{5} \frac{\partial \bar{\alpha}}{\partial F_z} = \frac{3}{5} \sum_i \beta_{iiz} \quad (2)$$

The values obtained with DFT and MSINDO geometries are listed in Table 4. Comparing the $\bar{\beta}$ values for DFT geometries and MSINDO geometries, it is apparent that the geometry dependence is here much more pronounced than for the $\bar{\alpha}$ values. The maximum difference is 9.58 au for imidazole.

We explain the sequence of $\bar{\beta}$ values for thiophene, pyrrole, and furan by location of net charges on the heteroatom X. S is positive, NH almost neutral, and O negative. Upon substitution of CH by N in the ring, the resonance effect (Figure 3) induces formally an $X^+ \rightarrow N^-$ charge separation, which leads to a further shift into the negative value region. This effect is distance-dependent and is enhanced for larger distances. Consequently, the $\bar{\beta}$ value is more negative for thiazole and imidazole than for isothiazole and pyrazole, respectively. The situation is reversed for X = O because oxygen resists the trend to acquire a positive charge via resonance stabilization.

For the diazoles and thiazoles a similar explanation can be used. For thiadiazoles and triazoles the sequence is

$$1,3,4 < 1,2,3 < 1,2,4 < 1,2,5$$

and can be explained by the distance dependence of the separated charges in the resonance structures. The situation is changed for oxadiazoles to

$$1,2,3 < 1,2,5 < 1,2,4 < 1,3,4$$

TABLE 4. Average First Hyperpolarizabilities $\bar{\beta}$ [au]^c of Azoles with DFT and MSINDO Optimized Geometries

	DFT geometries	MSINDO geometries
thiophene	34.40	26.00
	36.16 ^a	
thiazole	-97.42	-93.18
isothiazole	-35.96	-35.35
pyrrole	6.49	10.47
imidazole	-76.77	-67.19
pyrazole	-35.67	-35.56
furan	-33.17	-35.97
	-33.44 ^b	
oxazole	-5.26	0.93
isoxazole	-51.76	-54.79
thiadiazoles		
1,3,4-	-153.98	-157.44
1,2,4-	-53.68	-52.90
1,2,5-	6.98	0.70
1,2,3-	-93.14	-90.48
triazoles		
1H-1,3,4-	-88.82	-86.74
1H-1,2,4-	-34.43	-35.57
1H-1,2,5-	-12.41	-17.74
1H-1,2,3-	-77.61	-73.21
oxadiazoles		
1,3,4-	-3.41	-6.20
1,2,4-	-15.11	-16.53
1,2,5-	-39.18	-42.86
1,2,3-	-41.85	-47.44

^a $\bar{\beta}(-\omega; \omega, 0)$, $\lambda = 790$ nm, pure vibrational contribution 1.64 au. ^b $\bar{\beta}(-\omega; \omega, 0)$, $\lambda = 790$ nm, pure vibrational contribution -3.79 au. ^c 1 au = 8.63993×10^{-33} esu = 3.20662×10^{-53} C³·m³/J².

and bears some similarity to the reversal of the sequence of oxazole and isoxazole.

3.4. Second Hyperpolarizabilities. Second hyperpolarizabilities are calculated as

$$\bar{\gamma} = \frac{1}{5} \sum_{ij} \gamma_{ijij} \quad (3)$$

The static values obtained with DFT and MSINDO geometries are listed in Table 5. The trends are shown in Figure 6. Our values for thiophene and furan show good agreement with newer experimental values recently reported⁸ together with ab initio data. An older experimental value⁴¹ for thiophene is much smaller. It was measured with degenerate four-wave mixing (DFWM) and we cannot compute such values to comment on the experimental value.

To understand the trend for second hyperpolarizabilities, we followed the same line of argument as in previous work on azabenzenes.¹¹ From the calculated atomic hyperpolarizability values, $\bar{\gamma}_S = 9519$ au, $\bar{\gamma}_C = 3475$ au, $\bar{\gamma}_N = 718$ au, and $\bar{\gamma}_O = 567$ au, it is possible to conclude that $\bar{\gamma}$ values for azoles cannot be explained by atomic contributions. The large difference between $\bar{\gamma}_S$ and $\bar{\gamma}_N$ and between $\bar{\gamma}_N$ and $\bar{\gamma}_C$ is not reflected in the azole $\bar{\gamma}$ trend. As in the case of azabenzenes, an improvement would be the consideration of fragments which model the various types of ring bonds: C-S, N-S, C-C, C-N, N-N, C-O, N-O. The calculated values for the model fragments are the following: 11734 au for CH₂S, 9023 au for HNS, 8254 au for C₂H₄, 8244 au for CH₂NH, 7052 au for N₂H₂, 5972 au for CH₂O, and 5879 au for HNO. Here, the differences between the various model fragments are remarkably reduced compared to the atomic differences. These fragments are systems with two π electrons. If one wants to account for the fact that the heteroatom X contributes two π electrons, the following fragments would be more suitable: CH₂SH (26607 au), NHSH

TABLE 5. Average Second Hyperpolarizabilities $\bar{\gamma}$ [au]^d of Azoles with DFT and MSINDO Optimized Geometries

	DFT geometries	MSINDO geometries	experiment
thiophene	23349.08 28953.90 ^c	23336.45	8139 ^a 26206 ^b
thiazole	23579.40	23298.78	
isothiazole	19527.15	20291.27	
pyrrole	25935.09	25065.90	
imidazole	25949.19	24964.07	
pyrazole	18243.89	17889.83	
furan	16455.30 20697.50 ^c	15669.37	14889 ^b
oxazole	14020.18	13122.78	
isoxazole	11973.58	11945.02	
thiadiazoles			
1,3,4-	20045.36	20200.18	
1,2,4-	16604.49	17134.80	
1,2,5-	15013.36	16244.22	
1,2,3-	20071.45	22996.86	
triazoles			
1H-1,3,4-	20515.80	19444.82	
1H-1,2,4-	15575.81	15586.55	
1H-1,2,5-	13053.79	13013.66	
1H-1,2,3-	18182.91	18438.20	
oxadiazoles			
1,3,4-	10464.30	10009.87	
1,2,4-	9149.80	9188.19	
1,2,5-	8636.66	8835.91	
1,2,3-	9536.88	10000.87	

^a Reference 41. ^b Reference 8. ^c Pure electronic contribution to the optical Kerr effect, $\bar{\gamma}(-\omega; \omega, \omega, -\omega)$, determined by using the scaling relation (4). ^d 1 au = 5.03717×10^{-40} esu = 6.23597×10^{-65} C⁴·m⁴/J³.

(11489 au), CH₂NH₂ (126666 au), NHNH₂ (26683 au), CH₂-OH (23791 au), NHOH (5484 au). The systems are radicals with three π electrons.

The trend in Figure 6 can be commented upon with the following observations:

(1) The increment system of fragments governs the hyperpolarizabilities. Substitution of CH by N does not automatically lower the $\bar{\gamma}$ value because the C–C and C–N fragment have similar $\bar{\gamma}$ values. However, substitution of C–C by N–N does because the latter $\bar{\gamma}$ value is substantially lower. Isomers follow the increment system most closely.

(2) An increasing number of resonance structures increases the $\bar{\gamma}$ value. In the case of equal increment values, the larger number of resonance structure is more favorable.

(3) The increment system based on CH₂S and CH₂NH cannot explain the larger $\bar{\gamma}$ value of pyrrole compared to thiophene. The fragments CH₂SH and CH₂NH₂ are more suitable. But no quantitative increment system can be derived. An increment system which involves fragments with three ring atoms such as H₂CSCH₂, H₂CNHCH₂, and so forth would be better. However, this is too complicated to be useful.

Hieringer et al.⁴⁶ performed a basis set study for the second hyperpolarizability of furan. They used basis sets of quadrupole- ζ and double- ζ , in the valence and core regions, respectively. Their best result for furan is $\bar{\gamma}(0;0,0,0) = 12930$ au. This has been computed with a QZP+2d basis set and the GRAC potential. The CCSD(T) value reported by Kamada et al.⁸ is 14750 (6-31G+pdd). Our proposed electronic contribution for furan (16455.3 au; Table 5) is in reasonable agreement with both these estimates.

As has been stated, the polarizability and hyperpolarizability results, which have been discussed, are static. For completeness and to facilitate comparison with experiment, we have also computed some frequency-dependent property values for

The general trend for γ (DFT) is:

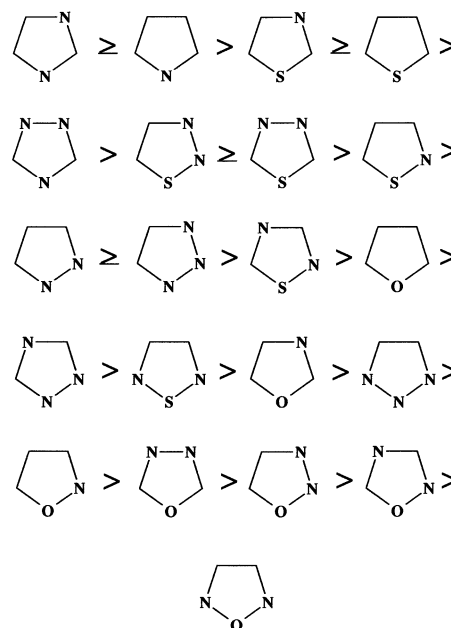


Figure 6. Trend of second hyperpolarizabilities.

thiophene and furan. Various authors, including Sekino and Bartlett,¹⁹ Rice and Handy,⁴⁷ and Pluta and Sadlej,⁴⁸ have demonstrated that reasonable estimates of frequency-dependent properties can be determined from eq 4:

$$P[\mathbf{M}(\omega)] = \{P[\text{SCF}(\omega)]/P[\text{SCF}(0)]\}P[\mathbf{M}(0)] \quad (4)$$

where $P[\text{SCF}(\omega)]$ and $P[\text{SCF}(0)]$ denote dynamic and static property values, computed using time-dependent Hartree–Fock (TDHF)⁴⁹ and Hartree–Fock theory, respectively, while $P[\mathbf{M}(\omega)]$ and $P[\mathbf{M}(0)]$ are the corresponding dynamic (estimated) and static (calculated) property values. Dalskov et al.⁵⁰ extensively discussed the range of applicability of the scaling procedure (eq 4), as well as its additive counterpart, for taking into account dispersion. In this work the scaling method has been used to find the frequency-dependent properties at the DFT level. In Table 5 we cited the second hyperpolarizability values of thiophene and furan, measured by using optically heterodyned optical Kerr effect experiments. Thus, we have computed $\bar{\gamma}(-\omega; \omega, \omega, -\omega)$ as well as $\bar{\alpha}(-\omega; \omega)$ and $\bar{\beta}(-\omega; \omega, 0)$. Both calculated and experimental values were determined at $\lambda = 790$ nm.⁸ The frequency-dependent polarizabilities and hyperpolarizabilities are given in Tables 3–5. It is observed that the computed and experimental $\bar{\alpha}(-\omega; \omega)$ and $\bar{\gamma}(-\omega; \omega, \omega, -\omega)$ are in reasonable agreement. The experimentally and theoretically determined $\bar{\gamma}(-\omega; \omega, \omega, -\omega)$ correspond to the electronic contributions.⁸ Zhao et al.⁴¹ measured the orientationally averaged second hyperpolarizability of thiophene, using degenerate four-wave mixing (DFWM) of tetrahydrofuran (THF) solutions.⁴¹ They found $\gamma = 8139$ au (at $\lambda = 632.8$ nm). The discrepancy observed between our value and that reported by Zhao et al. apparently is due to the different NLO procedure employed (it is known that the NLO properties greatly depend on the process⁵¹ and the environmental effects). In addition, the value reported by Zhao et al. has been measured in solution, while our value has been computed considering an isolated molecule; that is, no environmental interactions are taken into account. The scaled hyperpolarizability values for thiophene and furan are larger than the experimental values given in ref 8. Two

results are not adequate to define a trend. However, application to carefully selected molecules, for which reliable experimental data are available, may indicate possible ways for its improvement. To the best of our knowledge, no experimental first hyperpolarizability values for the considered molecules are available.

4. Vibrational Contributions for Azoles

The clamped nucleus approximation, which assumes the sequential application of the electric field to the electronic and nuclear motion, allows the resolution of the electric properties to electronic (P^e) and vibrational contributions.^{52,53} The vibrational property has two contributions: one is due to zero-point-vibrational-averaging, P^{zpv} and the other is the so-called pure vibrational term, P^{pv} . Thus, the total property P^t is given by the sum

$$P^t = P^e + P^{zpv} + P^{pv} \quad (5)$$

The pv and zpv contributions to the polarizabilities and hyperpolarizabilities are given by^{54–57}

$$\alpha^{pv} = [\mu^2]^{(0,0)} + [\mu^2]^{(2,0)} + [\mu^2]^{(1,1)} + [\mu^2]^{(0,2)} \quad (6)$$

$$\beta^{pv} = [\mu\alpha]^{(0,0)} + [\mu\alpha]^{(2,0)} + [\mu\alpha]^{(1,1)} + [\mu\alpha]^{(0,2)} + [\mu^3]^{(1,0)} + [\mu^3]^{(0,1)} \quad (7)$$

$$\gamma^{pv} = [\alpha^2]^{(0,0)} + [\alpha^2]^{(2,0)} + [\alpha^2]^{(1,1)} + [\alpha^2]^{(0,2)} + [\mu\beta]^{(0,0)} + [\mu\beta]^{(2,0)} + [\mu\beta]^{(1,1)} + [\mu\beta]^{(0,2)} + [\mu^2\alpha]^{(1,0)} + [\mu^2\alpha]^{(0,1)} + [\mu^4]^{(2,0)} + [\mu^4]^{(1,1)} + [\mu^4]^{(0,2)} \quad (8)$$

$$P^{zpv} = [P^e]^{(1,0)} + [P^e]^{(0,1)} \quad (9)$$

$$[P^e]^{(0,1)} = -\frac{\hbar}{4} \sum_{\alpha} \frac{1}{\omega_{\alpha}^2} \left(\sum_b \frac{F_{abb}}{\omega_b} \right) \left(\frac{\partial P^e}{\partial Q_{\alpha}} \right) \quad (10)$$

and

$$[P^e]^{(1,0)} = -\frac{\hbar}{4} \sum_{\alpha} \frac{1}{\omega_{\alpha}} \left(\frac{\partial^2 P^e}{\partial Q_{\alpha}^2} \right) \quad (11)$$

where ω_{α} is the harmonic frequency, F_{abb} is the cubic force constant, and Q_{α} is the normal coordinate. Analytical expressions for $[A]^{n,m}$ are given,⁵⁴ while n and m are the orders of the electrical and mechanical anharmonicity, respectively. The order of the derivatives, which have been taken into account in the present study, is given in parentheses: potential energy (4), dipole moment (3), polarizability (2), and first hyperpolarizability (1). These derivatives have been computed analytically.^{58,59} Details for the procedure, which was followed, have been given elsewhere.^{51,60}

The zpv corrections have been computed for the dipole moment and the polarizability. For P^{zpv} , first- and second-order derivatives of the corresponding electronic properties are required according to eqs 8–10. Analytic second-order derivatives are available only for the dipole moment and the polarizability. Numerical evaluation of the second-order derivatives of β^e and γ^e is, computationally, very expensive and usually unstable. Thus, we restricted our P^{zpv} properties to the dipole moment and the polarizability. The pv contributions have been computed for the polarizability and hyperpolarizabilities. Only properties of order equal or higher than 2 have a pv contribution.

We acknowledge that the vibrational properties should be computed with the method that was used for the calculation of the electronic properties. However, the TZV FIP2 basis set, which was used for the calculation of the γ^e values, would involve a computational cost for the calculation of the property derivatives, which is prohibitive. Thus, we have used the Pol basis set,⁶¹ at the SCF level, for the calculation of the vibrational properties since at this level analytical derivatives are available. The Pol basis sets for C, N, and O involve [10s6p4d/5s3p2d], while for H use [6s4p/3s2p]. They were derived using the basis set polarization method, which is related to the Hellmann–Feynman theorem.⁶¹ We have shown that the vibrational properties are less sensitive to the basis set than their electronic counterparts.^{11,51,62,63} These findings have been confirmed by the present work. It will be demonstrated and discussed in the next section that the Pol basis sets give vibrational property values, which do not have significant differences from those produced by the basis sets TZVP FIP1 and TZVP FIP2, which have been used for the computation of the electronic properties. Considering pyrrole as an example, we note that TZVP FIP2 and Pol have 250 and 175 functions, respectively. It is added that the computation of analytic derivatives of the properties, which are used for the calculation of the vibrational properties, is extremely demanding in terms of computing time for the size and number of molecules considered in this work. Using these findings, we have chosen to use for the computation of the electronic polarizabilities and hyperpolarizabilities the TZVP FIP basis sets, while for the vibrational properties the Pol sets are considered adequate. According to the theory we employ for the computation of the vibrational properties, the required property derivatives should be computed at the equilibrium geometry, which corresponds to the chosen method, that is, Pol/SCF. The vibrational properties have been computed using CADPAC,^{58,59} SPECTRO,⁶⁴ and Gaussian 98.²²

Most of the vibrational property values are static; that is, time-independent electric fields are considered. Static vibrational properties are much larger than the dynamic ones, and they are more interesting to discuss because they reveal in a more pronounced way specific aspects of the vibrational structure. However, some selected frequency-dependent property values will also be presented to facilitate comparison of our results with the experimental data. In Table 6 we present the vibrational contributions to the dipole moment, polarizability, and first and second hyperpolarizabilities of the considered compounds. We will first discuss the zpv corrections to μ and α and subsequently the pv contributions to α , β , and γ .

4.1. zpv Corrections. We first comment on the zpv corrections to the dipole moment and the polarizability. We note that

$$P^{zpv} = \langle 0|P^e(R)|0\rangle - P^e(R_e) \quad (12)$$

where $|0\rangle$ and R_e denote the ground-state vibrational wave function and the equilibrium geometry, respectively. The μ^{zpv} values of the considered compounds are very small. The smallest μ^{zpv} value has been observed for furan (0.001 au). The other computed μ^{zpv} values are in the range

$$0.01 \leq |\mu^{zpv}| \leq 0.041$$

The very small μ^{zpv} corrections do not affect the good agreement that exists between the computed electronic (DFT) and the experimental dipole moment values (Table 2).

TABLE 6. Vibrational Contributions to the Dipole Moment $\mu^{z\text{pva}}$, Polarizability $\bar{\alpha}^{z\text{pva}}$ and $\bar{\alpha}^{\text{pv}}$, First and Second Hyperpolarizabilities, $\bar{\beta}^{\text{pv}}$ and $\bar{\gamma}^{\text{pv}}$, Respectively, in au^a

molecule	$\mu^{z\text{pva}}$	$\alpha^{z\text{pva}}$	α^{pv}	β^{pv}	γ^{pv}
thiophene	-0.010	1.46	2.85	3.6	5417
thiazole	-0.010	1.16	2.62	-70.3	4152
isothiazole	-0.020	1.16	2.58	13.9	3514
pyrrole	-0.024	1.51	7.37	-305.1	25588
imidazole	-0.035	1.26	6.47	-257.4	15782
pyrazole	-0.018	1.24	5.77	-49.7	14493
furan	-0.001	1.34	3.51	-11.7	5102
oxazole	-0.013	1.06	2.99	-32.5	3194
isoxazole	-0.010	1.03	2.73	14.2	3046
thiadiazoles					
1,3,4-	-0.018	0.89	1.93	-30.0	2761
1,2,4-	-0.005	0.87	2.54	21.5	2403
1,2,5-	-0.015	0.87	2.48	29.5	1997
1,2,3-	-0.016	0.88	2.26	-37.4	4208
triazoles					
1H-1,3,4-	-0.041	0.99	6.10	-286.8	14057
1H-1,2,4-	-0.024	0.97	5.63	-166.9	11307
1H-1,2,5-	0.011	0.96	4.37	161.7	10857
1H-1,2,3-	-0.029	0.97	4.26	-63.5	7435

^a The computations have been performed with the Pol basis set at the SCF level.

The computed $\bar{\alpha}^{z\text{pba}}$ obey the following relationships:

two heteroatoms:

$$1.03 \leq \bar{\alpha}^{z\text{pva}} \leq 1.51$$

triazoles:

$$0.96 \leq \bar{\alpha}^{z\text{pva}} \leq 0.99$$

thiadiazoles:

$$0.87 \leq \bar{\alpha}^{z\text{pva}} \leq 0.89$$

The $\bar{\alpha}^{z\text{pva}}$ correction is small in comparison to α^{c} ; for example, it is 2.4% and 2.9% of α^{c} for thiophene and furan, respectively. The $\bar{\alpha}^{z\text{pva}}$ values should be taken into account when computed values are compared to the experimental ones. However, in the present case the observed good agreement between the calculated and the experimental data (Table 3) is not going to be substantially affected.

4.2. α^{pv} Contributions. In all the considered cases we observe that (Table 6)

$$\bar{\alpha}^{\text{pv}} > \bar{\alpha}^{z\text{pva}}$$

A similar trend has been found in our recent study of azabenzene.¹¹ Pyrrole, imidazole, pyrazole, and triazoles have considerably larger $\bar{\alpha}^{\text{pv}}$ values than the other azoles. All these compounds have in common the N–H group. To avoid the presentation of too many numerical data, we concentrate our analysis on pyrrole. The other derivatives with the N–H group follow the same pattern. Pyrrole was selected as a test case because, although there are numerous studies on its vibrational and electronic structure,^{65,66} there are still aspects that have not been considered in the literature. In the following the molecular plane of pyrrole is the yz plane and the dipole moment is oriented along the z axis. It is observed (Table 7) that α_{xx}^{pv} is much larger than the α_{yy}^{pv} and α_{zz}^{pv} components. The dominant contribution to α_{ii}^{pv} is made by $[\mu^2]^{(0,0)}$. This implies that the polarizability components, and in particular α_{xx}^{pv} and α_{yy}^{pv} , could be very well described by the double-harmonic approximation. The $[\mu^2]^{(0,0)}$ contribution to α_{xx}^{pv} was computed by using various

TABLE 7. Analysis of the Pure Vibrational Contribution to the Polarizability Components [au] of Pyrrole

	α_{xx}^{pv}	α_{yy}^{pv}	α_{zz}^{pv}		α_{xx}^{pv}	α_{yy}^{pv}	α_{zz}^{pv}
$[\mu^2]^{(0,0)}$	17.13	0.69	1.66				
	16.70 ^a			$[\mu^2]^{(2,0)}$	-0.88	0.19	0.40
	16.42 ^b			$[\mu^2]^{(1,1)}$	0.49	-0.03	0.41
	15.69 ^c			$[\mu^2]^{(0,2)}$	1.81	0.02	0.20
	16.42 ^d			α_{ii}^{pv}	18.55	0.87	2.67
	17.61 ^e				17.82 ^e		
	19.23 ^f				19.05 ^f		

^a Basis set: TZVP FIP1.¹⁷ Method: DFT. ^b Basis set: TZVP FIP2.¹⁷ Method: DFT. ^c Basis set: aug-cc-pVDZ.⁶⁷ Method: MP2. ^d Basis set: Pol. Method: MP2. ^e Basis set: 6-31G.⁶⁸ Method: SCF. ^f Basis set: 6-31++G**.⁶⁸ Method: SCF.

TABLE 8. Harmonic Vibrational Frequencies ω [cm⁻¹] of Pyrrole

sym.	ω		sym.	ω		sym.	ω	
	SCF	exp ^a		SCF	exp ^a		SCF	exp ^a
a_1	959.74	880	a_1	3914.21	3527	b_1	1576.36	1424
a_1	1091.33	1018	a_2	673.97	618	b_1	1712.06	1521
a_1	1142.63	1074	a_2	824.83	712	b_1	3376.6	3116
a_1	1246.37	1148	a_2	1063.4	868	b_1	3407.02	3140
a_1	1526.9	1391	b_1	937.6	863	b_2	494.01	474
a_1	1622.77	1470	b_1	1142.0	1049	b_2	685.05	626
a_1	3388.8	3125	b_1	1227.05	1134	b_2	833.94	720
a_1	3410.7	3148	b_1	1407.06	1287	b_2	999.78	826

^a The property values are those cited by Simandiras et al.⁶⁹

basis sets (e.g., Pol, TZVP FIP2 etc.^{17,61,67,68}), at the SCF, DFT, and MP2 levels of theory, to document the adequacy of the employed method (Pol/SCF) for the specified task. It is observed that there is satisfactory agreement between the Pol/SCF results and those given by TZV FIP2/DFT, as well as the other employed methods. By comparing the Pol/SCF and Pol/MP2 results, we deduce that correlation at the MP2 level has a small effect on $[\mu^2]^{(0,0)}$.

The size of the pure vibrational contribution relates to the vibrational (harmonic) frequencies of the molecules. It is observed that the Pol/SCF harmonic frequencies are in reasonable agreement with the experimental ones⁶⁹ (Table 8). It is thus expected that the Pol/SCF vibrational properties will, at least, present the correct trends.

Analysis of $[\mu^2]^{(0,0)}$ via eq 13,

$$\alpha_{ij}^{\text{pv}} = [\mu^2]^{(0,0)} = \sum_{\alpha} \frac{\left(\frac{\partial \mu_i^{\text{c}}}{\partial Q_{\alpha}} \right)_0 \left(\frac{\partial \mu_j^{\text{c}}}{\partial Q_{\alpha}} \right)_0}{\omega_{\alpha}^2} \quad (13)$$

for pyrrole has shown that the observed property, 17.1 au (Table 7), is due to two, mainly, vibrational modes, that is, those with frequencies 494.01 cm⁻¹ (10.30 au) and 833.94 cm⁻¹ (6.82 au). These are associated with the N–H and C–H wagging motions, respectively.^{70,71} The property value in parentheses denotes the contribution to $\alpha_{xx}^{\text{pv}}([\mu^2]^{(0,0)})$, associated with the specified mode.

We have also made some test computations on the saturated analogue of pyrrole, that is, C₄NH₉, using the 6-31G/SCF method. The trend found in pyrrole has confirmed that this derivative has $\alpha_{zz}^{\text{pv}}([\mu^2]^{(0,0)}) = 26.89$ au and most of this property (92.6%) is due to the wagging motion of N–H. Comparing the results for C₄NH₅ and C₄NH₉, we deduce that conjugation reduces the contribution of the N–H motion.

TABLE 9. Analysis of the Pure Vibrational Contribution to the First Hyperpolarizability Components [au] of Pyrrole^e

	β_{xxx}^{pv}	β_{yyz}^{pv}	β_{zzz}^{pv}		β_{xxx}^{pv}	β_{yyz}^{pv}	β_{zzz}^{pv}
$[\mu\alpha]^{(0,0)}$	28.50	3.37	0.18	$[\mu^3]^{(0,1)}$	-213.06	-0.78	-2.41
	29.64 ^a			$[\mu^3]^{(1,0)}$	-307.33	0.78	-5.56
	21.11 ^b			$[\mu\alpha]^{(1,1)}$	-13.32	2.35	-2.00
	28.45 ^c			$[\mu\alpha]^{(2,0)}$	-0.81	-1.94	-13.57
	29.13 ^d			$[\mu\alpha]^{(0,2)}$	6.48	1.77	8.84
				β_{iiz}^{pv}	-499.54	5.55	-14.52

^a Basis set: TZVP FIP1.¹⁷ Method: DFT. ^b Basis set: Pol. Method: MP2. ^c Basis set: TZVP FIP2.¹⁷ Method: DFT. ^d Basis set: 6-31G.⁶⁸ Method: SCF. ^e The computations have been performed with the Pol basis set, unless otherwise specified.

Dynamic vibrational contributions are much smaller (in fact, very often they are negligibly small), than the static ones because the optical frequencies are much larger than the harmonic frequencies. This trend is confirmed by the results of pyrrole, for which it has been found that $\bar{\alpha}^{pv}(-\omega;\omega) = -0.06$ au at $\lambda = 1064$ nm (method: Pol/SCF), as well as those of thiophene and furan (Table 3). These results suggest that the dynamic α^{pv} contribution will have a negligible effect and thus the good agreement between the computed and the experimental polarizabilities will not be affected (Table 3).

4.3. β^{pv} Contributions. Various methods (e.g., Pol/SCF, Pol/MP2, 6-31++G**/SCF) have been used for the computation of $[\mu\alpha]^{(0,0)}$ (double-harmonic approximation) to verify the adequacy of the Pol/SCF method and to examine the sensitivity of the results to the basis set and method variation. All the employed techniques gave similar results (Table 9). In particular, one notes the good agreement between the Pol/SCF and the TZV FIP2/DFT results. It is observed that correlation at the Pol/MP2 level reduces the $[\mu\alpha]^{(0,0)}$ value.

In general, the β^{pv} contributions are of comparable magnitude to β^e of the considered azoles (Tables 4 and 6). There are several cases in which the β^{pv} is, at least, an order of magnitude larger in absolute value than the corresponding β^e . Pyrrole, which has the larger $|\beta^{pv}|$, will be taken as an example to comment on the terms contributing to its β^{pv} . β_{xxx}^{pv} is the dominant component and the main contribution comes from $[\mu^3]^{(0,1)}$ and $[\mu^3]^{(1,0)}$. The first of those is determined in terms of the first-order dipole moment derivatives and the cubic force constants, while $[\mu^3]^{(1,0)}$ is computed in terms of the first- and second-order dipole moment derivatives. β_{yyz} and β_{zzz} are at least an order of magnitude smaller than β_{xxx}^{pv} (in absolute value). The anharmonicity of β_{xxx}^{pv} , which is expressed by the large values of $[\mu^3]^{(1,0)}$ and $[\mu^3]^{(0,1)}$ (-307.33 and -213.06 au, respectively), is attributed, mainly, to the NH group. This point is strengthened by noting that $[\mu^3]^{(1,0)}$ and $[\mu^3]^{(0,1)}$ for furan take the values -10.12 and 3.52 au, respectively. Similar small values are computed for thiophene (-12.39 au and 5.66 au, respectively).

Some dynamic property values for pyrrole have also been computed. These are $\beta^{pv}(-\omega;\omega, 0) = 2.7$ au (Pockels effect) and $\beta^{pv}(-2\omega;\omega,\omega) = -1.9$ au (second-harmonic generation), at $\lambda = 1064$ nm (method: Pol/SCF). These are comparable with the static electronic contribution (6.49 au; Table 4). The $\beta^{pv}(-\omega;\omega, 0)$ values of thiophene and furan are given in Table 4. These are relatively small in comparison to the corresponding electronic contributions, but not negligible. Overall, our results suggest that the dynamic β^{pv} should be taken into account when one aims at accurate results.

4.4. γ^{pv} Contributions. From the results of Tables 5 and 6, we observe that, in general, $\bar{\gamma}^{pv}$ is smaller than β^e , but both properties have a comparable magnitude. The larger $\bar{\gamma}^{pv}$ value has been found for pyrrole, which is used as an example to

TABLE 10. Analysis of the Pure Vibrational Contribution to the Second Hyperpolarizability Components of Pyrrole^e

	γ_{xxxx}^{pv}	γ_{yyyy}^{pv}	γ_{zzzz}^{pv}	γ_{xxzz}^{pv}	γ_{yyzz}^{pv}	γ_{xyyz}^{pv}
$[\mu\beta]^{(0,0)}$	2366.3	447.0	33.3	1894.3	-178.5	2918.0
$[\alpha^2]^{(0,0)}$	686.3	4937.6	3059.7	499.8	1074.3	704.8
	717.4 ^a	4969.2 ^a	2969.6 ^a	342.9 ^a	1038.3 ^a	554.9 ^a
	528.2 ^b	4324.8 ^b	3396.8 ^b	471.4 ^b	1242.3 ^b	593.0 ^b
	399.3 ^c	4302.5 ^c	3464.1 ^c	405.7 ^c	1251.4 ^c	466.2 ^c
	442.7 ^d	4418.7 ^d	3507.9 ^d	410.7 ^d	1262.8 ^d	509.0 ^d
$[\mu^2\alpha]^{(1,0)}$	2576.5	393.2	94.9	7011.2	-86.8	1821.9
$[\mu^2\alpha]^{(0,1)}$	-5118.9	-4.9	208.1	-5397.1	2.4	-2941.4
$[\alpha^2]^{(1,1)}$	1.5	30.8	-98.6	-4.1	-3.1	2.3
$[\mu\beta]^{(1,1)}$	6.3	-6.2	-56.1	42.7	-13.6	38.9
$[\mu^4]^{(1,1)}$	15319.4	-6.8	24.5	27382.8	0.02	-509.2
$[\mu\beta]^{(0,2)}$	3200.1	-40.2	20.6	-1559.1	25.5	-848.4
$[\mu\beta]^{(2,0)}$	-61.6	-5.5	-3.3	-46.3	-8.1	-85.6
$[\alpha^2]^{(0,2)}$	-38.5	-289.3	-271.1	18.2	-80.9	-35.5
$[\alpha^2]^{(2,0)}$	15.7	271.6	517.5	29.1	82.5	27.9
$[\mu^4]^{(0,2)}$	-1268.5	-0.3	23.2	9191.1	6.6	7.5
$[\mu^4]^{(2,0)}$	-25034.7	36.9	53.1	21306.0	-9.7	679.3
γ_{ijij}^{pv}	-73501	5763.9	3606.8	60368.6	810.6	1780.5

^a Basis set: 6-31++G**.⁶⁸ Method of computation: SCF. ^b Basis set: Pol. Method: MP2. ^c Basis set: TZVP FIP1. Method: DFT. ^d Basis set: TZVP FIP2. Method: DFT. ^e The computations have been performed using the Pol basis set, unless otherwise specified. The property values are in atomic units.

make a detailed analysis of the pure vibrational contribution. First, we report results that demonstrate the adequacy of the Pol/SCF approach. Various methods including the TZV FIP2/DFT and Pol/MP2, besides the Pol/SCF, have been used for the computation of the $[\alpha^2]^{(0,0)}$ contribution to $\gamma_{\alpha\alpha\beta\beta}^{pv}$ for pyrrole. The obtained results are in reasonable agreement with those computed using the Pol/SCF method. In particular, one notes the very good agreement between the Pol/SCF and TZV FIP2/DFT results for the property $\bar{\gamma}^{pv}([\alpha^2]^{(0,0)})$.

The largest component of $\bar{\gamma}^{pv}$ (pyrrole; Table 10) is γ_{xxzz}^{pv} . This is at least an order of magnitude larger than most of the other components. The larger terms contributing to γ_{xxzz}^{pv} are the $[\mu^4]^{(1,1)}$ and $[\mu^4]^{(2,0)}$. The first of these is determined in terms of the cubic force constant and the dipole moment derivatives (first and second order), while $[\mu^4]^{(2,0)}$ is computed using dipole moment derivatives (first, second, and third order).

To analyze the results of Table 10, we define

$$[A]^0 = [\mu\beta]^{(0,0)} + [\alpha^2]^{(0,0)}$$

$$[A]^1 = [\mu^2\alpha]^{(1,0)} + [\mu^2\alpha]^{(0,1)}$$

$$[A]^{\text{II}} = [\alpha^2]^{(2,0)} + [\alpha^2]^{(1,1)} + [\alpha^2]^{(0,2)} + [\mu\beta]^{(2,0)} + [\mu\beta]^{(1,1)} + [\mu\beta]^{(0,2)} + [\mu^4]^{(2,0)} + [\mu^4]^{(1,1)} + [\mu^4]^{(0,2)}$$

For the components γ_{yyyy}^{pv} , γ_{zzzz}^{pv} , γ_{xyyz}^{pv} , and γ_{yyzz}^{pv} , it has been found that

$$[A]^0 > |[A]^1| > [A]^{\text{II}}$$

For the components γ_{xxxx}^{pv} and γ_{xxzz}^{pv} , which are the larger ones, the following relationship has been found:

$$|[A]^{\text{II}}| > [A]^0 > [A]^1$$

In this case $|[A]^{\text{II}}|$ makes by far the larger contribution, in particular for γ_{xxzz}^{pv} . This indicates that the higher order terms are also likely to be of some importance.

It is essential to understand how the employed derivatives affect the properties of interest. Thus, we have taken as an example the α_{xx}^{pv} , β_{xxz}^{pv} , and γ_{xxzz}^{pv} components of pyrrole because

TABLE 11. Analysis of the Effect of the Various Property Derivatives on α_{xx}^{pv} , β_{xxz}^{pv} , and γ_{xxxz}^{pv} of Pyrrole (All in au)^a

<i>mnop</i>	α_{xx}^{pv}	β_{xxz}^{pv}	γ_{xxxz}^{pv}	<i>mnop</i>	α_{xx}^{pv}	β_{xxz}^{pv}	γ_{xxxz}^{pv}
0100	17.13	0.0	0	1221	38.82	-482.76	60338
0200	17.14	-307.33	21068	1321	37.92	-482.29	60529
0210	17.14	-278.83	21041	2100	18.93	-213.06	21068
0220	17.14	-279.11	28608	2200	19.45	-520.39	57642
0221	17.14	-279.11	30503	2210	19.45	-484.32	52236
0321	16.25	-279.64	30694	2220	19.45	-499.00	59799
1200	38.82	-520.39	57224	2221	19.45	-499.00	60177
1100	38.30	-213.06	8773	2320	18.55	-499.54	60037
1210	38.82	-468.08	51579	2321	18.55	-499.54	60368
1220	38.82	-482.76	59323				

^a Property values have been obtained with Pol basis set at the SCF level.

they are the larger ones and thus any effect is likely to be pronounced (Table 11). The anharmonicity will be described by *mnop*,⁷¹ where *m*, *n*, *o*, and *p* define the order of the potential energy (2–4), dipole moment (0–3), polarizability (0–2), and first hyperpolarizability derivatives (0,1), respectively. It is observed that the cubic force constant has a great effect on all properties [(0200)/(1200)], but the quartic force constant has a large effect only on α_{xx}^{pv} . The great effect of the second-order dipole moment derivatives on β_{xxz}^{pv} and γ_{xxxz}^{pv} is observed (e.g., (2100)/(2200)). The effect of the third-order dipole moment derivatives on α_{xx}^{pv} is small [(0221)/(0321)]. A similar observation is made by comparing the pairs: (1221)/(1321) and (2221)/(2321). In fact, these derivatives reduce α_{xx}^{pv} by approximately the same amount (≈ 1 au). Similarly, the above derivatives have a very small effect on β_{xxz}^{pv} and γ_{xxxz}^{pv} . Noticeable is the effect of the first- and second-order polarizability derivatives on β_{xxz}^{pv} and γ_{xxxz}^{pv} [(1200)/(1210)]. Negligible is the effect of the first-order derivatives of β^e on γ_{xxxz}^{pv} [(2320)/(2321)]. This justifies the approximation to neglect the second-order derivatives of β^e .

The present work is, primarily, interested in the analysis of the static property values. However, for completeness, we also present some dynamical values for pyrrole, that is, $\bar{\gamma}^{pv}(-\omega; \omega, 0, 0) = 3207$ au (dc-Kerr effect), $\bar{\gamma}^{pv}(-2\omega; \omega, \omega, 0) = 382$ au (dc-field induced second-harmonic generation) and $\bar{\gamma}^{pv}(-3\omega; \omega, \omega, \omega) = -37$ au (third-harmonic generation), at $\lambda = 1064$ nm (method:Pol/SCF). For thiophene it has been found that $\bar{\gamma}^{pv}(-\omega; \omega, 0, 0) = 1785$ au at $\lambda = 709$ nm. This value corresponds to 8% of the corresponding static electronic contribution (Table 5). The great dependence of γ^{pv} on the nonlinear optical process is clearly seen, as well as the dramatic decrease of the dynamic value, in comparison to that, which corresponds to the static limit (Table 6). However, the value of $\bar{\gamma}^{pv}(-\omega; \omega, 0, 0)$, is not negligible and should be taken into account for proper comparison with the experimental values.

Kamada et al.⁸ have measured $\bar{\gamma}(-\omega; \omega, \omega, -\omega)$ of thiophene and furan. We report both the pure vibrational and electronic contributions for the above process, at $\lambda = 790$ nm. The latter are shown in Table 5, while the computed pure vibrational contributions to the above property are 1833.6 au for thiophene and 1570.7 au for furan.

For completeness we note that the study of the vibrational properties has been greatly facilitated by the pioneering work of Bishop and Kirtman.^{54,55} Most of the studies in the literature follow in some form their perturbation approach, although the finite perturbation theory approach by Cohen et al. has also been used.⁷² Particular attention has been paid to model studies of small molecules.⁵⁶ Very few, relatively larger, molecules (e.g., C₆H₆,⁷³ C₆H₅NH₂⁷⁴) have been considered and most of these at

a very approximate level. Among these studies we note the work of Millefiori and Alparone,⁷⁵ who have calculated the vibrational polarizabilities and first hyperpolarizabilities of C₄H₄X (X = O, S, Se, Te), using several basis sets at the double-harmonic approximation.

5. Conclusion

A DFT method has been used to compute the dipole moments, polarizabilities, and hyperpolarizabilities for thiophene, pyrrole, furan, and their respective azoles, diazoles, and triazoles. Their geometries have been optimized by employing the DFT and MSINDO techniques. The observed trends have been explained by an interplay between atomic contributions, distance-dependent charge separation between heteroatoms, and number of resonance structures. A similar explanation can be provided for the electronic first hyperpolarizabilities. The corresponding electronic second hyperpolarizabilities follow a trend determined by incremental contributions from bond fragments and number of resonance structures. Exceptions from the increment scheme are observed for thiophene and pyrrole and their azoles with nonadjacent substitution to the heteroatom. To explain these, fragments with pairs of adjacent ring bonds have to be considered.

The vibrational contribution to the dipole moments, polarizabilities, and hyperpolarizabilities of the above compounds has also been computed using the Pol/SCF method. Several techniques (basis sets and approaches to take into account electron correlation) have been used to confirm the adequacy of the employed method. The zpva corrections to the dipole moment and the polarizability have also been taken into account. The static vibrational polarizabilities of several of the considered compounds are small, but not negligible. Relatively larger vibrational polarizabilities have been computed for the derivatives, which involve the N–H functional group. Detailed analysis has been performed on pyrrole, which was taken as an example of the above derivatives, and it has been found that the large vibrational polarizability is associated, primarily, with the N–H wagging motion. Large contribution has also been observed for the C–H wagging motion. The static vibrational polarizabilities and hyperpolarizabilities are of comparable magnitude to the electronic ones. These have been rationalized by using the property derivatives, in terms of which these are determined. A limited analysis on the dynamic vibrational properties of pyrrole was also conducted to facilitate comparison with the experimental property values.

There are very few experimental or theoretical studies on the nonlinear optical properties of most of the considered compounds, although some of those are fundamental units of important conjugated polymers (e.g., pyrrole/polypyrrole).

One may add that several computational studies have been reported in the literature on the properties of five-membered heteroatomic rings, the most relevant of which have been cited and discussed. However, these works have focused on the electronic contributions to the polarizabilities and hyperpolarizabilities. The novelties of this study are the following: (i) Both electronic and vibrational contributions are considered. Besides the work of Millefiori and Alparone,⁷⁵ who considered the pure vibrational contributions to the first hyperpolarizability of furan and thiophene, at the double-harmonic approximation, to the best of our knowledge, no other calculations have been reported on the zpva correction and the pure vibrational contributions of the examined compounds. (ii) It is systematic, since 22 compounds are treated at a uniform level of approximation. This allows discussion of the structure–polariza-

tion relationship of azoles in a comprehensive way (four properties are treated and all significant contributions are taken into account). (iii) The interpretation scheme we employ is different from that used by other teams. In particular, we note that El-Bakali Kassimi et al., who have undertaken a systematic study of the electronic polarizabilities of 10 azoles⁵ and 10 oxazoles,⁶ used some empirical formulas relying on atom- and bond-additive models.

Acknowledgment. This work was partially supported by the European Commission via the TMR network DELOS. P.C. gratefully acknowledges computer time from CSCA-CINVESTAV and partial support by CINVESTAV via JIRA Grant Nos. 000264 and 000268 as well as by CONACYT Project Nos. 36037-E.

Supporting Information Available: Six tables of structural data. This material is available free of charge via the Internet at <http://pubs.acs.org>.

References and Notes

- Katritzky, A. R. *Handbook of Heterocyclic Chemistry*; Pergamon Press: Oxford, 1985.
- Nalwa, H. S.; Miyata, S. *Nonlinear Optics of Organic Molecules and Polymers*; CRC Press: Boca Raton, FL, 1997.
- Sutherland, R. L. *Handbook of Nonlinear Optics*; Marcel Dekker: New York, 1996.
- Keshari, V.; Wijekoon, W. M. K. P.; Prasad, P. N.; Karna, S. P. *J. Phys. Chem.* **1995**, *99*, 9045.
- El-Bakali Kassimi, N.; Doerksen, R. J.; Thakkar, A. J. *J. Phys. Chem.* **1995**, *99*, 12790.
- El-Bakali Kassimi, N.; Doerksen, R. J.; Thakkar, A. J. *J. Phys. Chem.* **1996**, *100*, 8752.
- El-Bakali Kassimi, N.; Lin, Z. *J. Phys. Chem. A* **1998**, *102*, 9906.
- Kamada, K.; Ueda, M.; Nagao, H.; Tawa, K.; Sugeno, T.; Shmiru, Y.; Ohta, K. *J. Phys. Chem. A* **2000**, *104*, 4723.
- Calaminici, P.; Jug, K.; Köster, A. M. *J. Chem. Phys.* **1998**, *109*, 7756.
- Calaminici, P.; Jug, K.; Köster, A. M. *J. Chem. Phys.* **1999**, *111*, 4613.
- Calaminici, P.; Jug, K.; Köster, A. M.; Ingamells, V. E.; Papadopoulos, M. *J. Chem. Phys.* **2000**, *112*, 6301.
- Köster, A. M.; Krack, M.; Leboeuf, M.; Zimmermann, B. AL-LCHEM, Universität Hannover, 1998.
- Godbout, N.; Salahub, D. R.; Andzelm, J.; Wimmer, E. *Can. J. Phys.* **1992**, *70*, 560.
- Köster, A. M. Habilitation Thesis, Universität Hannover, 1998.
- Krack, M.; Köster, A. M. *J. Chem. Phys.* **1998**, *108*, 3226.
- Vosko, S. H.; Wilk, L.; Nusair, M. *Can. J. Phys.* **1980**, *58*, 1200.
- Zeiss, G. D.; Scott, W. R.; Suzuki, N.; Chong, D. P.; Langhoff, S. R. *Mol. Phys.* **1979**, *37*, 1543.
- van Gisbergen, S. J. A.; Snijders, J. G.; Baerends, E. J. *J. Chem. Phys.* **1998**, *109*, 10657.
- Sekino, H.; Bartlett, R. J. *J. Chem. Phys.* **1993**, *98*, 3022.
- Aiga, F.; Tada, T.; Yoshimura, R. *J. Chem. Phys.* **1999**, *111*, 2878.
- Kurtz, H. A.; Stewart, J. J. P.; Dieter, K. M. *J. Comput. Chem.* **1990**, *11*, 82.
- Frisch, M. J.; Trucks, G. W.; Schlegel, H. B.; Scuseria, G. E.; Robb, M. A.; Cheeseman, J. R.; Zakrzewski, V. G.; Montgomery, J. A., Jr.; Stratmann, R. E.; Burant, J. C.; Dapprich, S.; Millam, J. M.; Daniels, A. D.; Kudin, K. N.; Strain, M. C.; Farkas, O.; Tomasi, J.; Barone, V.; Cossi, M.; Cammi, R.; Mennucci, B.; Pomelli, C.; Adamo, C.; Clifford, S.; Ochterski, J.; Petersson, G. A.; Ayala, P. Y.; Cui, Q.; Morokuma, K.; Malick, D. K.; Rabuck, A. D.; Raghavachari, K.; Foresman, J. B.; Cioslowski, J.; Ortiz, J. V.; Stefanov, B. B.; Liu, G.; Liashenko, A.; Piskorz, P.; Komaromi, I.; Gomperts, R.; Martin, R. L.; Fox, D. J.; Keith, T.; Al-Laham, M. A.; Peng, C. Y.; Nanayakkara, A.; Gonzalez, C.; Challacombe, M.; Gill, P. M. W.; Johnson, B. G.; Chen, W.; Wong, M. W.; Andres, J. L.; Head-Gordon, M.; Replogle, E. S.; Pople, J. A. *Gaussian 98*, revision A.2; Gaussian, Inc.: Pittsburgh, PA, 1998.
- Ahlsweide, B.; Jug, K. *J. Comput. Chem.* **1999**, *20*, 563.
- Ahlsweide, B.; Jug, K. *J. Comput. Chem.* **1999**, *20*, 572.
- Ahlsweide, B. Ph.D. Thesis, Universität Hannover, 1998.
- Nanda, D. N.; Jug, K. *Theor. Chim. Acta* **1980**, *57*, 95.
- Landolt-Börnstein. *Zahlenwerte und Funktionen aus Naturwissenschaften und Technik*; NS II/7; Springer: Berlin, 1976.
- Christen, D.; Griffith, J. H.; Sheridan, J. Z. *Naturforsch.* **1981**, *36a*, 1378.
- Kumar, A.; Sheridan, J.; Stiefvater, O. L. *Z. Naturforsch.* **1978**, *33a*, 145.
- Stiefvater, O. L. *J. Chem. Phys.* **1975**, *63*, 2560.
- Stiefvater, O. L. *Z. Naturforsch.* **1976**, *31a*, 1681.
- Stiefvater, O. L. *J. Chem. Phys.* **1976**, *13*, 73.
- Bolton, K.; Brown, R. D.; Burden, F. R.; Mishra, A. *J. Mol. Struct.* **1975**, *27*, 261.
- McClellan, A. L. *Tables of Experimental Dipole Moments*; Rahara Enterprises: El Cerrito, CA, 1974; Vol. 2.
- McClellan, A. L. *Tables of Experimental Dipole Moments*; W.H. Freeman: San Francisco, CA, 1963.
- Katritzky, A. R. *Physical Methods in Heterocyclic Chemistry*; Academic Press: New York, 1974; Vol. 6.
- Begtrup, M.; Nielsen, C. J.; Nygaard, L.; Samdal, S.; Sjøgren, C. E.; Sørensen, G. O. *Acta Chem. Scand.* **1988**, *A42*, 500.
- Bak, B.; Nielsen, J. T.; Nielson, O. F.; Nygaard, L.; Rastrup-Andersen, J.; Steiner, P. A. *J. Mol. Spectrosc.* **1996**, *19*, 458.
- Le Fèvre, C. G.; Le Fèvre, R. J. W.; Rao, B. P.; Smith, M. R. *J. J. Chem. Soc.* **1959**, 1188.
- Dennis, G. R.; Gentle, I. R.; Ritchie, G. L. D.; Andrieu, C. G.; *J. Chem. Soc., Faraday Trans. 2* **1983**, *79*, 539.
- Zhao, M. T.; Singh, B. P.; Prasad, P. N. *J. Chem. Phys.* **1988**, *89*, 5535.
- Coonan, M. H.; Craven, I. E.; Hesting, M. R.; Ritchie, G. L. D.; Spackman, M. A. *J. Phys. Chem.* **1992**, *96*, 7301.
- Calderbank, K. E.; Calvert, R. L.; Lukins, P. B.; Ritchie, G. L. P. *Aust. J. Chem.* **1981**, *34*, 1835.
- Perdew, J. P.; Wang, Y. *Phys. Rev. B* **1986**, *33*, 8800. Perdew, J. P. *Phys. Rev. B* **1986**, *33*, 8822.
- Becke, A. D. *Phys. Rev. A* **1988**, *38*, 3098; Lee, C.; Yang, W.; Parr, R. G. *Phys. Rev. B* **1988**, *37*, 785.
- Hieringer, W.; van Gisbergen, S. J. A.; Baerends, E. J. *J. Phys. Chem. A* **2002**, *106*, 10380.
- Rice, J. E.; Handy, N. C. *Int. J. Quantum Chem.* **1992**, *43*, 91. Rice, J. E. *J. Chem. Phys.* **1992**, *96*, 7580.
- Pluta, T.; Sadlej, A. J. *J. Chem. Phys.* **2001**, *114*, 136.
- Schmidt, M. W.; Baldridge, K. K.; Boatz, A. J.; Elbert, S. T.; Gordon, M. S.; Jensen, J. H.; Koseki, S.; Matsunaga, N.; Nguyen, K. A.; Su, S. J.; Windus, T. L.; Dupuis, M.; Montgomery, J. A. *J. Comput. Chem.* **1993**, *14*, 1347.
- Dalskov, E. K.; Jensen, H. J. A.; Oddershede, J. *Mol. Phys.* **1997**, *90*, 3.
- Ingamells, V. E.; Papadopoulos, M. G.; Raptis, S. G. *J. Chem. Phys. Lett.* **1999**, *307*, 484.
- Bishop, D. M.; Kirtman, B.; Champagne, B. *J. Chem. Phys.* **1997**, *107*, 5780.
- Perpète, E. A.; Champagne, B.; Jacquemin, D. *J. Mol. Struct. (THEOCHEM)* **2000**, *529*, 65.
- Bishop, D. M.; Luis, J. M.; Kirtman, B. *J. Chem. Phys.* **1998**, *108*, 10013.
- Bishop, D. M. *Adv. Chem. Phys.*; Prigogine, I., Rice, S. A., Eds.; Wiley: New York, 1998; Vol. 104, p 1.
- Bishop, D. M.; Norman, P. In *Handbook of Advanced Electronic and Photonic Materials*; Nalwa, H. S., Ed.; Academic Press: San Diego, CA, 2001; Vol. 9, p 1.
- Bishop, D. M.; Sauer, S. P. A. *J. Chem. Phys.* **1997**, *107*, 8502.
- Amos, R. D.; Alberts, I. L.; Andrews, J. S.; Colwell, S. M.; Handy, N. C.; Jayatilaka, D.; Knowles, P. J.; Kobayashi, R.; Koga, N.; Laidig, K. E.; Maslen, P. E.; Murray, C. W.; Rice, J. E.; Sanz, J.; Simandiras, E. D.; Stone, A. J.; Su, M.-D. *CADPAC5.0, The Cambridge Analytic Derivatives Package*; Cambridge, UK, 1992.
- Amos, R. D.; Alberts, I. L.; Andrews, J. S.; Colwell, S. M.; Handy, N. C.; Jayatilaka, D.; Knowles, P. J.; Kobayashi, R.; Koga, N.; Laidig, K. E.; Maslen, P. E.; Murray, C. W.; Rice, J. E.; Sanz, J.; Simandiras, E. D.; Stone, A. J.; Su, M.-D. *CADPAC6.0, The Cambridge Analytic Derivatives Package*, Cambridge, UK, 1995.
- Eckart, U.; Ingamells, V. E.; Papadopoulos, M. G.; Sadlej, A. J. *J. Chem. Phys.* **2001**, *114*, 735.
- Sadlej, A. J. *Collect. Czech. Chem. Commun.* **1988**, *53*, 1995.
- Ingamells, V. E.; Papadopoulos, M. G.; Handy, N. C.; Willetts, A. *J. Chem. Phys.* **1998**, *109*, 1845.
- Avramopoulos, A.; Papadopoulos, M. G. *Mol. Phys.* **2002**, *100*, 821.
- Willetts, A.; Gaw, J. F.; Green, W. H.; Handy, N. C. *SPECTRO Theoretical Spectroscopy Package*.
- Christiansen, O.; Gauss, J.; Stanton, J. F.; Jørgensen, P. *J. Chem. Phys.* **1999**, *111*, 525.
- Mellouki, A.; Liévin, J.; Herman, M. *J. Chem. Phys.* **2001**, *271*, 239.
- Dunning, T. H., Jr. *J. Chem. Phys.* **1989**, *90*, 1007.

- (68) Hehre, W. J.; Ditchfield, R.; Pople, J. A. *J. Chem. Phys.* **1972**, *56*, 2257.
- (69) Simandiras, E. D.; Handy, N. C.; Amos, R. D. *J. Phys. Chem.* **1988**, *92*, 1739.
- (70) Held, A.; Herman, M. *Chem. Phys.* **1995**, *190*, 407.
- (71) Xie, Y.; Fan, K.; Boggs, J. E. *Mol. Phys.* **1986**, *58*, 401.

- (72) Cohen, M. J.; Willetts, A.; Amos, R. D.; Handy, N. C. *J. Chem. Phys.* **1994**, *100*, 4467.
- (73) Magnoni, M. C.; Mondini, P.; Del Zoppo, M.; Castiglioni, C.; Zerbi, G. *J. Chem. Soc., Perkin Trans. 2* **1999**, 1.
- (74) Champagne, B. *Int. J. Quantum Chem.* **1997**, *65*, 689.
- (75) Millefiori, S.; Alparone, A. *Phys. Chem. Chem. Phys.* **2000**, *2*, 2495.